AFM monitoring of size changes during thermal syntheses of ferric oxide nanoparticles

M. Vůjtek[*,1], **R. Kubínek**[1], **R. Zbořil**[2], and **L. Machala**[1]

[1] Department of Experimental Physics, Palacký University, 17. listopadu 50, 771 46 Olomouc, Czech Republic
[2] Department of Physical Chemistry, Palacký University, Svobody 8, 771 46 Olomouc, Czech Republic

Thermal decomposition represents a simple and low-cost method of synthesis of nanoparticles. We have employed atomic force microscopy (AFM) to study the decomposition of Prussian Blue to amorphous ferric oxide. We have monitored the influence of the precursor particle size on the particle size of resultant Fe_2O_3 and we discuss the applicability of AFM and their agreement with other methods.

Keywords atomic force microscopy; nanoparticles; Fe_2O_3

1. Introduction

Ferric oxide is a unique polymorphic compound occuring in various structural forms, including amorphous and it is interesting from the viewpoints of the applied research and scientific research [1,2]. Thermally induced solid-state reaction of suitable Fe-precursors in combination with the post-processing (magnetic, dissolution, sedimentation) separation represent a simple and low-cost synthesis of Fe_2O_3 nanoparticles. If the chemical and structural composition of the powder is kept constant, two particle characteristics – morphology and size distribution – can greatly influence the applicability of iron oxide nanoparticles. The present paper demonstrates the use of AFM for monitoring particle size transformations during thermal decomposition of Fe-precursors to Fe_2O_3 nanophase.

2. Theoretical considerations

There are many methods used in the nanoparticle research for particle size and morphology evaluation and they constitute a great variety of physical principles with many advantages and drawbacks. Among them, transmission electron microscopy is the most extensively used experimental technique, which provides two-dimensional images of the particles. This method enables one to obtain general information on particle morphology and evaluate size distribution in two dimensions very precisely [3–6]. However, this method needs demanding sample preparation in order to prevent particle agglomeration and transfer into vacuum. Moreover, it is highly probable that the energy released from impinging electron beam can lead to an irreversible change of the particle size, and crystallization of the amorphous phase.

In recent years, AFM has been established as a complementary and very useful method for characterization of three-dimensional shapes in the "nanoworld" [7–11]. In comparison to TEM, the sample treatment is much easier and can be used in various environment including air and liquid. In addition, there is no problem with particle size changes or crystallization during the measurement. The AFM principle and sample preparation result in imaging well-dispersed and separated particles.

Unfortunately, lateral dimensions are influenced by so-called the tip-sample convolution, which considerably enlarges them within the range of a tip radius. The correction is made by "deconvolution" [12–15] process which requires an exact knowledge of a tip shape and size [16, 17]. Without this knowledge, the image is only improved partially and exact lateral dimensions can not be determined. It is obvi-

[*] Corresponding author: e-mail: milan.vujtek@upol.cz, Phone: +420585634950

ous that the lateral analysis of AFM images of particles smaller than a tip radius (approx. 10 nm) is pointless.

Many researchers compared results obtained by TEM and AFM and conclude the enlargement [18]. In the case of spherical particles, it was, however, shown that the mean lateral dimension, determined by TEM coincides with the mean vertical dimension determined by AFM very well, and the vertical dimension acquired with high precision was used for the analysis of the spherical particles [19]. Thus, in the case of the spherical particles, its vertical dimension is labeled as a particle size, e.g. we introduce an effective diameter as many other methods do. The spherical shape of the particles can be supported by the observed circular cross-sections and lateral widths comparable to a nominal tip radius, which limits the asymmetry of the particles to low values. AFM can be used even as a relative technique for characterization of thermal treatment of non-spherical particles if the particle aspect ratio can be assumed being constant.

3. Experimental details

3.1 Syntheses of precursors and ferric oxide nanopowders

Our experiment was performed with Prussian Blue as a precursor. We prepared the precursor by two different routes. The sample labeled `S' was prepared by thermally induced solid-state decomposition of ammonium ferrocyanide in air at 160 °C for 3 h; the residual ammonium was removed by dissolution in water and the oxide was then dried. The sample labeled `W' was synthesized by a "wet way" – the solution of potassium ferrocyanide was added to an excess of iron(III) chloride. Thermal decomposition of this two different samples (`S', `W') in air at 250 °C for 2 h results in samples labeled `S250' and `W250', respectively. X-ray and Mössbauer spectroscopy analyses show that both precursors are very clean crystalline Prussian Blue and resulting oxide is amorphous, well-stoichiometric Fe_2O_3.

3.2 AFM analysis of nanoparticles

AFM measurements were performed using an AFM Explorer microscope (ThermoMicroscopes, USA) in air and at room temperature, in a non-contact mode with Si cantilevers of a 1650-00 type (ThermoMicroscopes) with a nominal tip radius of 10 nm and resonant frequencies of about 220 kHz.

The image processing was carried out using a SPMLab software and includes plane levelling, background removing and occasional stripe removing. The determination of the particle height was carried out with external processing software. The height was determined as a difference between maximum height in the inner part of annulus and the average height in the area of annulus. Particles with noise spikes and obvious agglomerates were excluded from the analysis.

Analyzed iron oxides and Fe-precursors were dispersed in destilled and deionized water and ultrasonificated at a temperature of about 50 °C. Then, 20 µl of solution was spread on freshly cleaved mica substrate (Grade V-4, Structure Probe) and put into drying oven at 60 °C for 30 min, subsequently transfered into sample holder and immediatelly measured.

3.3 Complementary techniques

The transmission ^{57}Fe Mössbauer spectra were collected using a Mössbauer spectrometer with a ^{57}Co(Rh) source. Measurements were carried out at temperatures ranging from 5 to 300 K in zero external magnetic field. The phase composition of samples was monitored by XRD using a Seifert-FPM diffractometer with a CuKα radiation and conventional θ–2θ geometry. Si was used as an external calibration standard. The specific surface area of Fe_2O_3 powders was determined using a BET surface area analyzer Coulter SA 3100. The particle size distribution was obtained by dynamic light scattering (DLS)

method using a Particle size analyzer ZetaPlus 90. The HRTEM analysis was performed by a Phillips CM12 microscope equipped with an EDAX 9800 analyzer.

4. Results

4.1 Precursor analysis

The samples of Prussian Blue were investigated by DLS, XRD, TEM, and AFM in order to obtain the particle size information. DLS investigation shows a narrow distribution of both samples. In the case of sample `W', particle sizes are within the range of 56 to 66 nm, particles of `S' sample are smaller with diameters ranging from 18 to 29 nm. Both results were obtained from multimodal data processing. Similar results were obtained from TEM analysis, namely 60 to 70 nm for `W' particles and 20 to 35 nm for `S' sample, and XRD analysis, namely 68 nm for `W' particles and 31 nm for `S' particles.

The analysis of AFM images (Fig. 1) is rather more complicated. The assumption of spherical shape of Prussian Blue particles would lead to the conclusion that particles of sample `W' and `S' have a mean diameter of 31 nm and 11 nm, respectively. These values are significantly smaller than the values obtained by DLS and TEM. This difference can be therefore explained by a non-spherical shape of the particles. To verify this hypothesis, lateral dimensions (influenced by convolution) have to be investigated.

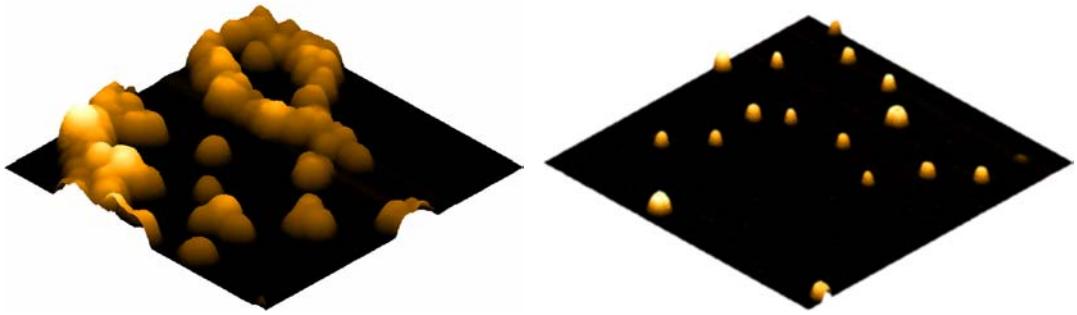

a) scan size 1200 nm, height 78 nm b) scan size 2000 nm, height 13.8 nm

Fig. 1 AFM image of sample a) `W', b) `S'.

The `W' particles show a strong tendency to agglomerate in a `chain-like' manner. It is known [20] that the convolution deformation is less pronounced in the direction of such chain, in comparison with that for an isolated particle. The analysis of valley-to-valley distances of line-profile along the line connecting adjacent particles (chain axis) shows a mean value of 50 nm. This value is relatively close to that obtained by DLS or TEM measurements. From the top-view image (not shown), it is clear that lateral dimensions of isolated particles are different in perpendicular directions and that the orientation of the longer axes is different for different particles. The last fact enables to exclude the possibility that the elongation is caused entirely due to a convolution artefact. The difference in lateral dimensions is approximately 15 nm. If we assume that the lateral dimension influenced by convolution cannot be smaller than the height of the particle (this assumption is supported by height vs. lateral dimension measurement on spherical latex particles), the sum of the above mentioned difference and the height of the particle results in the lower estimation of lateral particle size. In this case we obtain a value of approximately 50 nm, which agrees well with the valley-to-valley distances.

It can be assumed that isolated particles are predominantly oriented in parallel direction to the mica surface. On the other hand, particles in 2D agglomerates can have many orientations due to a mutual hindering. Therefore, the heights of images of agglomerated particles can vary in much broader range than those measured in the case of isolated particles. In the case of `W' particles, the measured heights range from 45 to 60 nm. From these results, we can conclude that `W' particles are non-spherical with

the longer axis of about 50 nm (the maximum height of 60 nm can exhibit the particles not touching the mica surface).

The image of `S' sample shows well-resolved individual particles with heights within the range of 7 to 16 nm. In the top-view image, all particles are highly symmetrical. Therefore, we cannot use the same procedure as discussed earlier. However, the ratio of the lateral and vertical dimensions differs even for particles with the same height. We found some particles with a height of approximately 11 nm and measured their lateral widths. The obtained values are as follows: $h_1 = 11.54$ nm, $w_1 = 73$ nm, $h_2 = 11.19$ nm, $w_2 = 94$ nm, $h_3 = 11.5$ nm and $w_3 = 67$ nm. Because of the nearly identical height and circular shape, the difference in widths (the largest value is 27 nm) cannot be attributed to the convolution. Thus, it can be stated that lateral dimensions of particles are at least 27 nm. This value is in accordance with DLS and TEM measurements.

Although the AFM height of particles is different from DLS and TEM diameters, we can remark that the ratio between dimensions of `W' and `S' particles is approximately the same for all methods. With regard to the above mentioned results, we can conclude that samples `W' and `S' differ in particle size and shape, but they have identical chemical composition and structure.

4.2 Amorphous ferric oxide analysis

Amorphous oxide `W250' was firstly investigated without ultrasonification, because of a discrepancy between results obtained by other methods of particle size characterization. The AFM image (Fig. 2) reveals highly symmetrical particles with lateral diameters of 100–150 nm. Particle profiles do not show any indication of agglomeration of particles, as a smooth line-profile with only one local maximum was measured for these particles. Another sample was prepared by ultrasonification and, as a result, very small particles were observed. Thus, we can state that the first analysis revealed agglomerates only and that this oxide exhibits a remarkable tendency to form uniformly sized and shaped agglomerates.

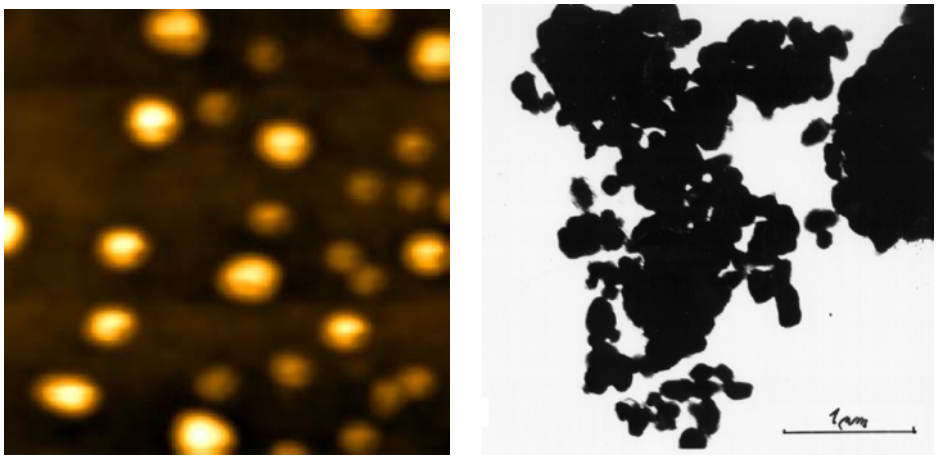

a) scan size 500 nm b)

Fig. 2 a) AFM and b) TEM image of `W250' prepared without an ultrasonification.

Subsequent samples were prepared by ultrasonification. TEM analysis revealed small particles in both samples, with dimensions of 3–4 nm for `W250' and 2–3 nm for `S250'. Because of limited XRD and DLS applicability, size of these particles was estimated from BET surface area γ; we obtained $\gamma_{W250} = 210$ m^2/g and $\gamma_{S250} = 415$ m^2/g. Due to the identical chemical composition, the ratio between specific areas is proportional to the inverse ratio between particle radii. Thus, we obtain $d_{W250} / d_{S250} = 1.98$.

The vertical size analysis of AFM images showed very small particles with narrow size distribution and their maxima were relatively shifted, from 3.1 nm for `W250' to 1.6 nm for `S250'. Because of the small size, the lateral analysis is not feasible and we cannot assess the particle morphology (the overall shape of the image is determined by the tip shape). However, particles with small dimensions are usually spherical.

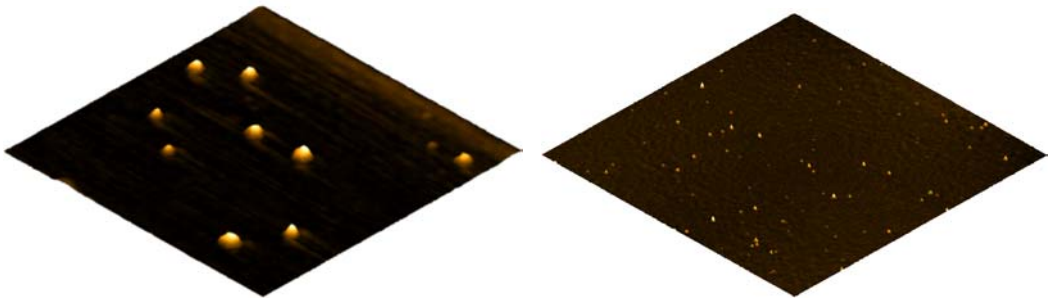

a) scan size 1270 nm, height 3.5 nm b) scan size 2000 nm, height 4 nm

Fig. 3 AFM image of sample a) `W250', b) `S250'.

4.3 Discusion

The height information from AFM images can be used as an exact particle diameter when spherical particles are investigated. Unfortunatelly, it was observed that Prussian Blue particles are highly non-spherical. This fact leads to a disagreement among AFM height measurements, TEM lateral measurement and DLS size distributions. The careful observation of particle shapes, study of their orientation to scanning axes, measurement of size in different directions and comparison of lateral dimensions of particles with approximately the same height can be used to overcome, to some extent, the convolution deterioration. After these corrections, a satisfactory degree of accordance among various methods has been improved.

On the other hand, the assumption of spherical shape of oxide nanoparticles is not in contradiction with experimental data because of consistence of TEM, AFM and BET measurements.

The structural and chemical methods have shown that both `W' and `S' samples are identical regarding their chemical composition and structure. The only differences represent the particle size – particles of sample `W' are approximately two times larger than `S' particles – and shape – `S' particles exhibit more circular cross-sections. The chemical composition and structure of both oxides `W250' a `S250' was also found to be the same. However, the difference in the particle size was preserved during the thermal decomposition. Therefore, we can conclude that there is a possibility to control the particle size of the resultant oxide by a change of the precursor particle size.

5. Conclusions

With regard to the investigation of Prussian Blue precursors and resultant oxides after thermal decomposition, we have shown that the choice of larger precursor particles leads to a formation of larger particles of iron oxide. We have demonstrated that AFM is an useful technique to study these transformations, even in the case of the non-spherical particles of the precursors.

Acknowledgements This work has been supported by the Ministry of Education of the Czech Republic, Research Center 1M6198959201.

References

[1] R. Zboril, M. Mashlan and D. Petridis, Chemistry of Materials **14**, 969 (2002).
[2] R. Zboril, M. Mashlan, K. Barcova and M. Vujtek, Hyperfine Interactions **139**, 597 (2002).
[3] L. Lacava, B. Lacava, R. Azevedo, Z. Lacava, N. Buske, A. Tronconi and P. Morais, Journal of Magnetism and Magnetic Materials **225**, 79 (2001).
[4] U. Lagerpusch, B. Anczykowski and E. Nembach, Philosophical Magazine A **81**, 2613 (2001).
[5] X. Zeng, N. Koshizaki and T. Sasaki, Applied Physics A **69**, S253 (1999).
[6] J.A. Derose and J.-P. Revel, Journal of Microscopy **195**, 64 (1999).
[7] M.R. Yalamanchili, S. Veeramasuneni, M.A.D. Azevedo and J.D. Miller, Colloids and Surfaces A **133**, 77 (1998).
[8] M. Rasa, B.W.M. Kuipers and A.P. Philipse, Journal of Colloidal and Interface Science **250**, 303 (2002).
[9] G.B. Khomutov, I.V. Bykov, R.V. Gainutdinov, S.P. Gubin, A.Y. Obydenov, S.N. Polyakov and A.L. Tolstikhina, Colloids and Surfaces A **198-200**, 347 (2002).
[10] D. Wei, R. Dave and R. Pfeffer, Journal of Nanoparticle Research **4**, 21 (2002).
[11] W. Lü, D. Yang, Y. Sun, Y. Guo, S. Xie and H. Li, Applied Surface Science **147**, 39 (1999).
[12] J.S. Villarrubia, Journal of Research of National Institute of Standards and Technology **102**, 425 (1997).
[13] D. Keller, Surface Science **253**, 353 (1991).
[14] K.I. Schiffmann, M. Fryda, G. Goerigk, R. Lauer and P. Hinze, Ultramicroscopy **66**, 183 (1996).
[15] D.Q. Yang, Y.Q. Xiong, Y. Guo, D.A. Da and W.G. Lu, Journal of Material Science **36**, 263 (2001).
[16] P.M. Williams, M.C. Davies, C.J. Roberts and S.J.B. Tendler, Applied Physics A **66**, S911 (1998).
[17] V.A. Bykov, Yu.A. Novikov, A.V. Rakov and S.M. Shikin, Ultramicroscopy **96**, 175 (2003).
[18] P. Mulvaney and M. Giersig, Journal of Chemical Society – Faraday Transactions **92**, 3137 (1996).
[19] G. Roe, L. McDonnell and A. Ghanem, Ultramicroscopy **100**, 319 (2004).
[20] A. Dias, V.T.L. Buono, J.M.C. Vilela, M.S. Andrade and T.M. Lima, Journal of Material Science **32**, 4715 (1997).